Control of Vibration and Noise- New Millennium:
International Mechanical Engineering Congress & Exposition
6th Biennial Symposium on Active Control of Vibration and Noise

Preliminary Performance Analysis of the Space Interferometer Mission Using an Integrated Modeling Methodology

Ipek Basdogan
ipek.basdogan@jpl.nasa.gov
(818) 354-0952

Robert Grogan
Robert.L.Grogan@jpl.nasa.gov
(818) 354-6927

Andy Kissil
akissil@mail1.jpl.nasa.gov
(818) 354-8479

Norbert Sigrist
sigrist@mail1.jpl.nasa.gov
(818) 354-1979

Lisa Sievers
lisa@grover.jpl.nasa.gov
(818) 353-1990

Jet Propulsion Laboratory,
California Institute of Technology
4800 Oak Grove Drive
Pasadena, CA 91109

ABSTRACT

Space Interferometer Mission (SIM) scheduled for launch in 2006, is one of the premiere missions in the Origins Program, NASA's endeavor to understand the origins of the galaxies, of planetary systems around distant stars, and perhaps the origins of life itself. The precise tolerance required by the SIM instrument facilitates the investigation of many design options, trades, and methods for minimizing interaction between the actively controlled optics and the structure. One of the complementary activities that addresses these technological challenges is the integrated modeling methodology development and validation at Jet Propulsion Laboratory. The methodology integrates structural, optical, and control system modeling into a common environment and enables end-to-end performance evaluation of the complex opto-mechanical systems.

This paper provides an overview of the integrated modeling methodology and introduces the most recent SIM Reference Design model. The SIM integrated model is used in system requirement trade studies and performance analysis to support the overall system design and ongoing error budget efforts.

Optical performance in interferometry is typically measured in terms of optical pathlength difference (OPD) and differential wavefront tilt (DWT). This paper focuses on the OPD performance metric and investigates the OPD jitter resulting from reaction wheel assembly (RWA) disturbances. RWA is the largest anticipated disturbance source on the spacecraft and assessing the impact of the wheel disturbance frequency contents and magnitude levels on the optical performance is essential for the success of the mission. Broadband and discrete frequency models of the TELDIX/RDR-68 reaction wheels are used to perform the disturbance analysis. The overall system design can benefit from such analysis results by identifying the critical regions in the frequency domain and decoupling the dynamics of the optical and structural components from the disturbance spectrum and the control bandwidth. The preliminary performance results show that the current SIM Reference Design meets the mission requirements for the overall wheel speeds. However, some of the modeling assumptions and component models must be validated by experimental studies before the subsystem requirements are finalized.

1. INTRODUCTION

Detection of earth-like planets around stars by measuring the stars motion requires an instrument with micro- arcsecond astrometric measurement accuracy [1]. Spaceborne optical interferometers are likely to be the first instrument class capable of achieving this accuracy level. Interferometry is a combined in order to achieve the equivalent resolution of a

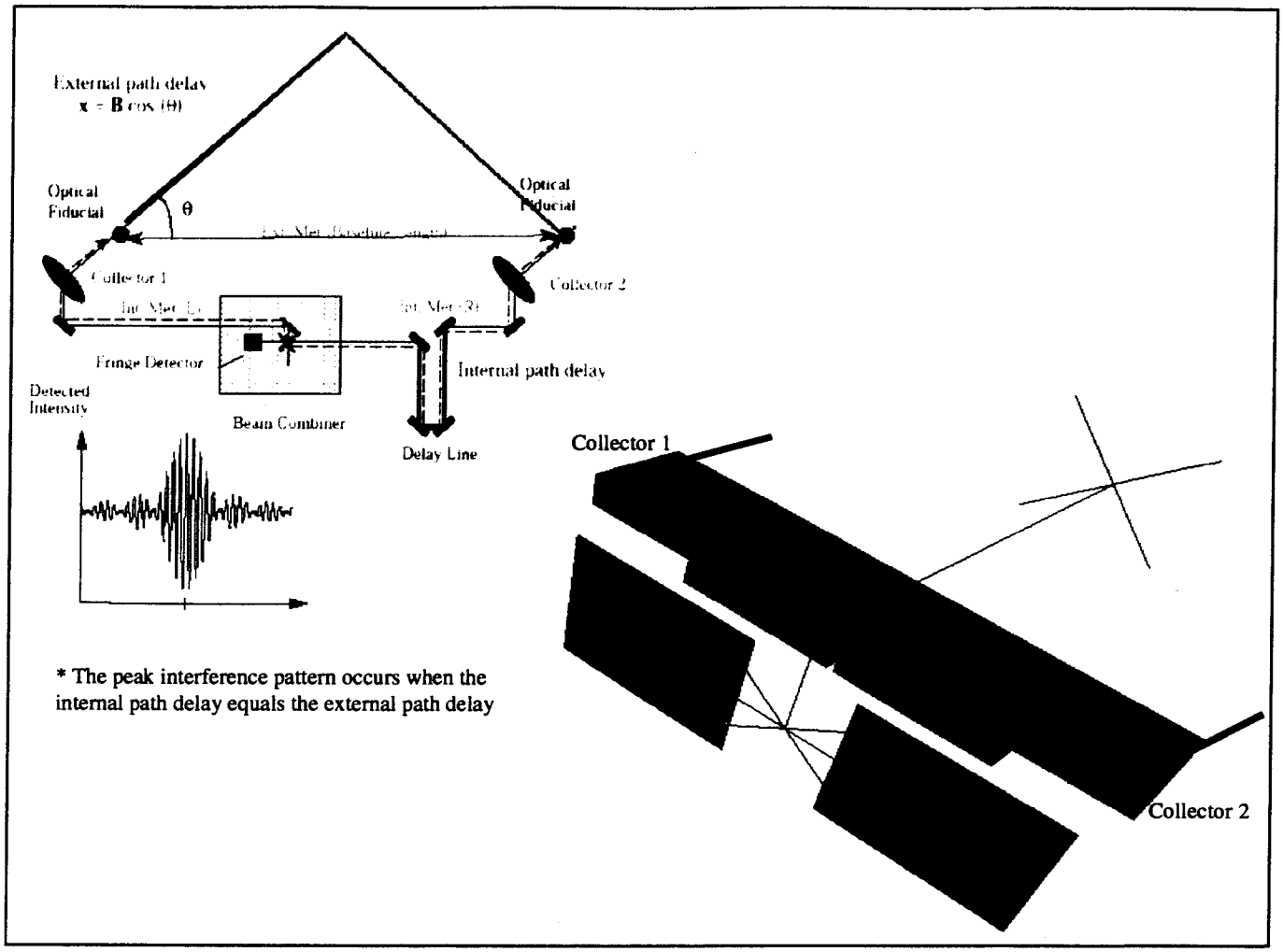

Figure 1 SIM Reference Design and interferometry concept.

technique in which the light from two collecting apertures are single telescope with a diameter equal to the separation distance of the two collecting apertures. When the light is combined properly it interferes and this can be detected in the form of an interference fringe. The resulting data, the fringe amplitudes, phases and positions may be used to measure the angular separation of multiple stellar objects. The Space Interferometry Mission (SIM) with a launch date in 2006 will serve as a science mission, as well as a technology pathfinder for future astrophysics missions providing a leap forward in space based astronomy beyond the Hubble Space Telescope. The instrument requires stabilization of the optical path lengths, where each optical path travels through one of the collecting apertures, to be equal down to the nanometer level, as well as laser metrology measurements of down to the tens of picometer [2]. Illustrated in Figure 1, the SIM Reference Design uses four collinear interferometers mounted on a 10-meter long boom. Each interferometer collects light from two collectors located at the right and left side of the boom and combines them in the center of the boom. Two of the four interferometers will acquire fringes on bright guide stars in order to make highly precise measurements of the spacecraft attitude. The third interferometer will observe the science targets and measure the target positions with respect to an astrometric grid of some 4000 stars evenly distributed around the celestial sphere (Note that the fourth interferometer serves as a backup if one of the other interferometers fails during the operation). The illustration of the interferometry concept given in Figure 1 shows that an optical external path delay (OPD) occurs when the starlight arrives the right collector sooner than the left collector. An internal path delay must be introduced to compensate for the external path delay to form the fringes. The equalization of the pathlength is accomplished by an actively controlled optical delay line located on one arm of the interferometer [3]. Once the delay line is set to a

position where the paths are exactly equal, the angle to the star can be

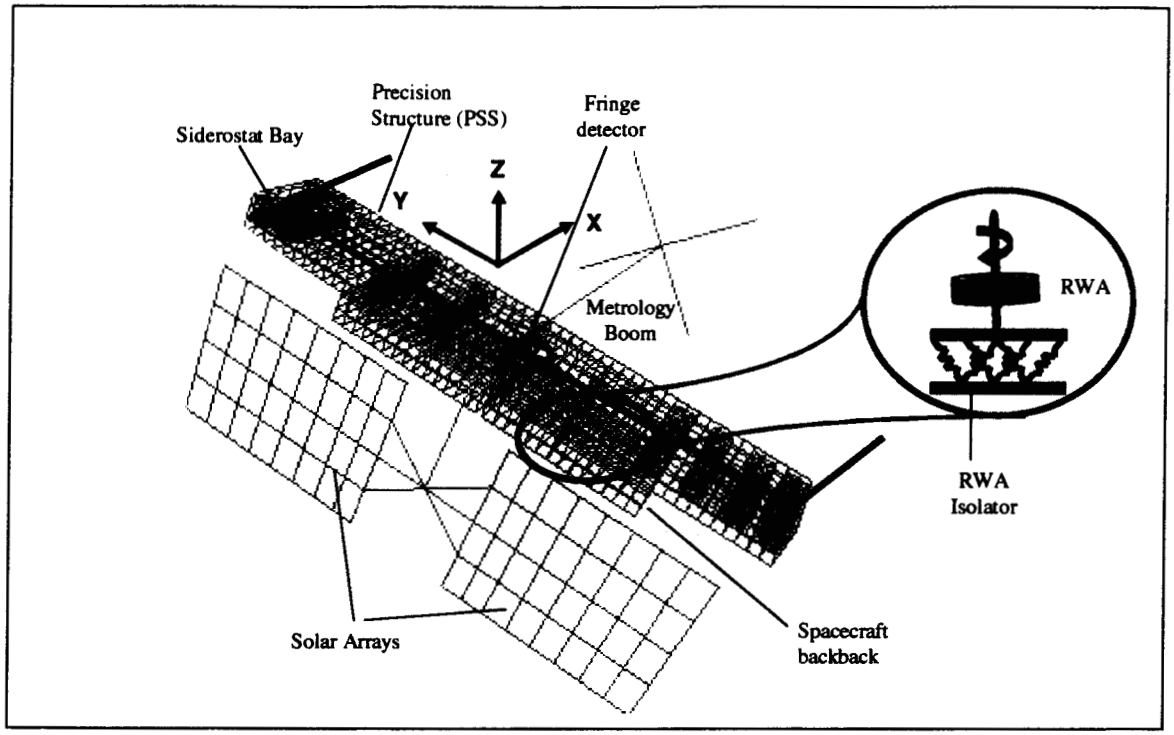

Figure 2 SIM Reference Design Integrated Model

determined by measuring optical pathlength in the interferometer. All these components form the fringe tracking subsystem and they stabilize the optical path difference (OPD) between the two telescopes or equivalently the stellar fringe position down to 10 nm (RMS) in the presence of the existing disturbances.

The largest anticipated disturbance source on SIM is the reaction wheel assembly (RWA). Reaction wheels are momentum exchange devices which are often used for spacecraft attitude control and performing large angle slewing maneuvers. The wheel disturbances can be classified by their frequency content, magnitude level, and location /direction at which they enter the structure. Especially for the pathlength control system, all these factors become crucial and must be quantified when such a high level precision is required for the success of the mission.

Accurate models of the instrument and the disturbance sources are necessary to predict the performance of the SIM Reference Design prior to building the flight system hardware. In anticipation of meeting these needs, an integrated modeling methodology that combines structural, optical, and control system design within a common software environment has been developed and validated as a part of Interferometry Technology Program (ITP) at JPL [4,5]. The methodology enables an end-to-end performance evaluation of the system requirements using an integrated opto-mechanical model. This model allows the calculation of the transfer functions from various inputs to various outputs using the state space approach lending itself most easily to analysis and control synthesis. Inputs are defined at the disturbance and the control actuator locations whereas the outputs are measured at the optical sensors. This study focuses only on the OPD performance prediction and studies the effect of the reaction wheel disturbances on the OPD jitter. After the transfer functions are obtained using the integrated model, disturbance analysis is performed using the disturbance model of the TELDIX/RDR-68 wheels. Following section provides an overview of the integrated methodology and introduces the structural, optical and disturbance models of the current SIM Reference Design.

2. SIM REFERENCE DESIGN INTEGRATED MODEL

The SIM Reference Design integrated model consists of a structural finite element model and a linear optical model integrated together. The structural model is generated with IMOS [6], whereas both IMOS and COMP [7] are used to create the optical model. The integration and disturbance analyses are performed in MATLAB with the aid of IMOS functions.

2.1 Structural Model

The structural model that comprises 27,000 degrees of freedom (dof), is specified in IMOS as a finite element geometry, shown in Figure 2. This geometry consists of plate, beam, and rigid body elements, modeling the spacecraft and the instruments. The components consist of precision structure (PSS), spacecraft and instrument backpacks, solar array, metrology boom, RWA isolators and the backpack isolators. Substructuring and component mode synthesis techniques are used to reduce the size of the finite element model to 1200 modes.

The governing equation for the multiple degree of freedom system generated by the finite element analysis is

$$\mathbf{M}\ddot{\mathbf{d}} + \mathbf{C}\dot{\mathbf{d}} + \mathbf{K}\mathbf{d} = \mathbf{F}\mathbf{u} \tag{1}$$

where $\mathbf{M}$, $\mathbf{K}$ and $\mathbf{C}$ are the mass, stiffness and damping matrices of the system. The vector $\mathbf{d}$ is the nodal displacements, $\mathbf{u}$ is the control input and $\mathbf{F}$ is the influence matrix for $\mathbf{u}$. Then the system in Eq. 1 is transformed to the modal coordinates as

$$\mathbf{\Phi}^{\mathrm{T}}\mathbf{M}\mathbf{\Phi}\,\ddot{\eta} + \mathbf{\Phi}^{\mathrm{T}}\mathbf{C}\mathbf{\Phi}\,\dot{\eta} + \mathbf{\Phi}^{\mathrm{T}}\mathbf{K}\mathbf{\Phi}\,\eta = \mathbf{\Phi}^{\mathrm{T}}\mathbf{F}\,\mathbf{u} \tag{2}$$

where $\mathbf{\Phi}$ is the modal transformation matrix and η is the vector of modal coordinates [8]. Equation 2 can then be rewritten as n uncoupled differential equations as

$$\ddot{\eta}_i + 2\zeta_i\omega_i\dot{\eta}_i + \omega_i^2\eta_i = f_i \qquad i = 1,2,...,n \tag{3}$$

where ζ_i is the modal damping factor, ω_i is the natural frequency of mode i, and n is the number of independent dof. The modal damping factor ζ_i is assumed to be 0.25 % for the global flexible-body modes and 10% for the dynamics associated with the delay line and isolator modes. These damping values are consistent with the estimates obtained from the modal tests [9].

2.2 Optical Model

The optical model begins with the prescription of the optical elements in all 4 interferometers. This prescription includes the shapes, positions, and orientations of the optical elements. A sample ray trace of the optical prescription is shown in Figure 2 overlapped with the finite element model of the system. Figure 2 also shows the location of the RWA disturbance input and the optical sensor (fringe detector) for the pathlength control system. This optical prescription together with the structural model is generated in IMOS based on the layout of the actual optical elements on SIM structure. Optical model generation uses the structural finite element geometry in order to simplify prescription definition and to ease the subsequent structural-optical model integration. This allows the location of optical elements to be measured with respect to reference points on the structure as opposed to with each other. Furthermore, structural nodes that correspond to optical element attachment points are easily identified or defined.

Once the optical prescriptions are specified, they are exported to COMP, where linear optical models are created. These linear models are calculated by performing an analytic differential ray trace [7]. The result is a model of the form:

$$\mathbf{y} = \mathbf{C}_{opt}\,\mathbf{d}_{opt} \tag{4}$$

where $\mathbf{d}_o$ is a vector of optical element perturbations (*i.e.*, a subset of $\mathbf{d}$ in Eq. 1), $\mathbf{y}$ is a vector of optical output, and $\mathbf{C}_{opt}$ is the optical sensitivity matrix giving the change in ray state due to perturbations of the optical elements. The optical output can be pathlength difference, wave front tip/tilt, or beam sheer depending on the analysis performed.

2.3 Structural-Optical Model

First, the structural model is truncated to remove modes above the bandwidth of expected disturbances (*i.e.* above 1000 Hz) [10]. Then, the structural and optical models are integrated to form a structural-optical model in first-order, state-space form, such that:

$$\begin{aligned} \dot{\mathbf{x}} &= \mathbf{A}\mathbf{x} + \mathbf{B}\mathbf{u} \\ \mathbf{y} &= \mathbf{C}\mathbf{x} \end{aligned} \tag{5}$$

where

$$\mathbf{A} = \begin{bmatrix} \mathbf{0} & \mathbf{I} \\ -\mathbf{M}_P^{-1}\mathbf{K}_P & -\mathbf{M}_P^{-1}\mathbf{C}_P \end{bmatrix}$$

$$\mathbf{B} = \begin{bmatrix} 0 \\ \mathbf{M}_P^{-1}\mathbf{F}_P \end{bmatrix} \qquad [\mathbf{C}] = [\mathbf{C}_{opt}\mathbf{\Phi} \quad \mathbf{0}]$$

State space form approach allows the calculation of the transfer functions that relates the output OPD, $\mathbf{Y}(\omega)$, to the given RWA disturbance inputs, $\mathbf{U}(\omega)$, such that

$$\mathbf{H}(\omega) = \frac{\mathbf{Y}(\omega)}{\mathbf{U}(\omega)} \tag{6}$$

Inputs are defined at disturbance locations and actuated degrees of freedom for the articulated optical surfaces whereas outputs are measured at the fringe detectors and wave front tilt cameras. The transfer functions for all disturbance directions are obtained using the standard MATLAB functions after the state space model is built.

Figure 5 shows the transfer function plot calculated from the RWA x-axis force disturbance input to OPD output.

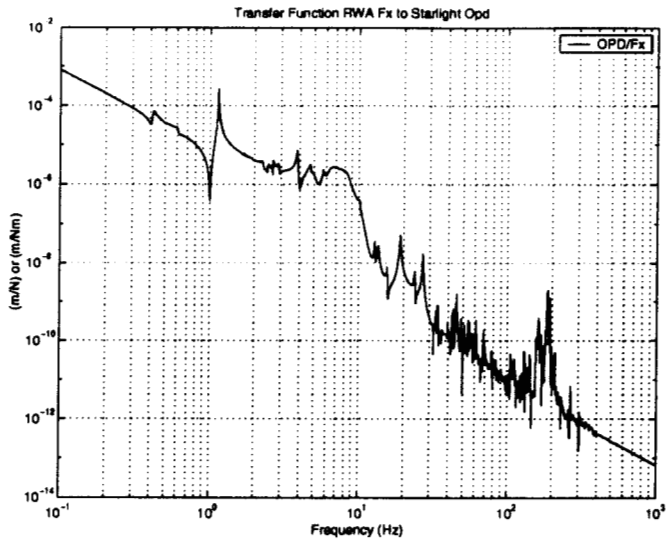

Figure 3 Transfer function from RWA force-x disturbance to OPD for the first interferometer (Collectors 1-2 pair)

2.4 Control Model

The interferometer requires a number of optical control systems in order to perform a measurement. These consist of pointing and pathlength control. While the pointing control system enable measurement of the interference fringe, it is the pathlength control system that directly controls the optical quantity of the stellar fringe. In particular, the purpose of the pathlength control system is to equalize stellar pathlength from the observed star through each arm of the interferometer to the detector (refer to Figure 1). The pathlength control system must stabilize this optical path difference down to 10 nm (RMS) in the presence of the reaction wheel disturbances. The closed loop configuration for the rest of the paper refers to the case where the loops are closed for the pathlength control system. Until the control system design for the mission is finalized, the pathlength control system is simulated by a 2nd order high pass filter in the analysis with a roll-off frequency at 100 Hz which is the estimated disturbance rejection capacity of the pathlength control system [10].

2.5 RWA Disturbance Model

After developing an integrated model of the system, the next step is to assess the performance of the instrument when the model is subjected to the anticipated disturbance sources. In this study, TELDIX/RDR-68 reaction wheel model is used to assess the effect of the disturbances on the OPD performance. The disturbance model was based on test data from eight TELDIX/RDR-68 RWA units conducted when the wheels were mounted to a rigid base [11]. The variation in disturbance amplitudes across the wheel set allows calculation of both a mean and max-expected disturbance for the wheel set. The max-expected case is selected for this study since it is a conservative model that provides an envelope of the disturbances generated by this particular wheel.

Based on the test data obtained from the TELDIX/RDR-68 units, disturbance forces and torques can be modeled as discrete harmonics of the reaction wheel speed, f_{rwa}, with amplitudes proportional to the square of the wheel speed [11, 12]

$$m(t) = \sum_{i=1}^{n} C_i f_{rwa}^2 \sin(2\pi h_i f_{rwa} t + \phi_i) \qquad (7)$$

where $m(t)$ is the disturbance torque or force, C_i is an amplitude coefficient, h_i is the harmonic number, and ϕ_i is a random phase (uniform over [0, 2π]). The model includes the axial force (along the wheel spin axis), two radial forces (normal to the spin axis), and two radial torques (causing wheel to wobble). Disturbance torque about the axis of rotation is considered to be insignificant. After the force and torque disturbance models are obtained, two analysis approaches have been followed for the integration of the wheel model with the transfer functions obtained from the SIM integrated model.

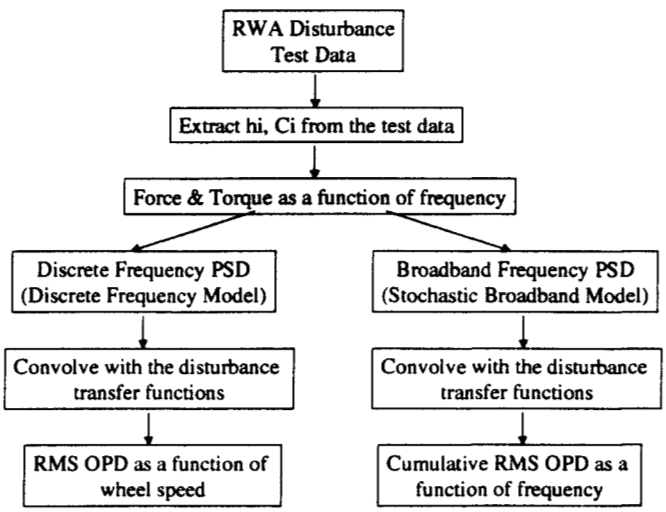

Figure 4 RWA Disturbance Analysis Approach

Discrete Frequency approach assumes that the power spectral densities (PSD) of the disturbance function consist of discrete impulses occurring at frequencies, $h_i f_{rwa}$, with

amplitude, $\frac{C_i^2 f_{rwa}^4}{2}$. As an example, Figure 5a shows the discrete frequency power spectral density (PSD) of the radial force where the TELDIX/RDR-68 wheel is spinning at 25 revolutions per second (rps).

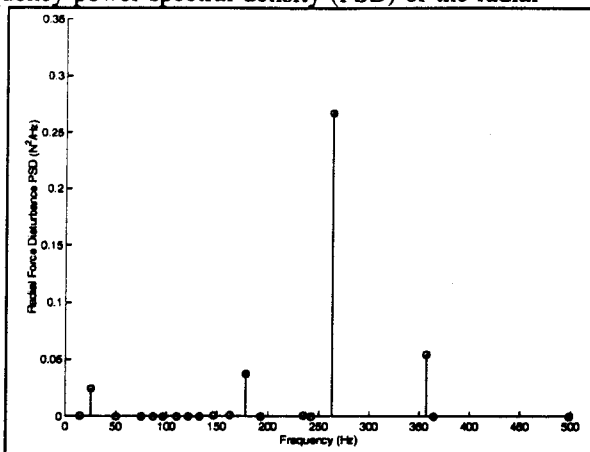

Figure 5a RWA discrete frequency PSD calculated at 25 rps.

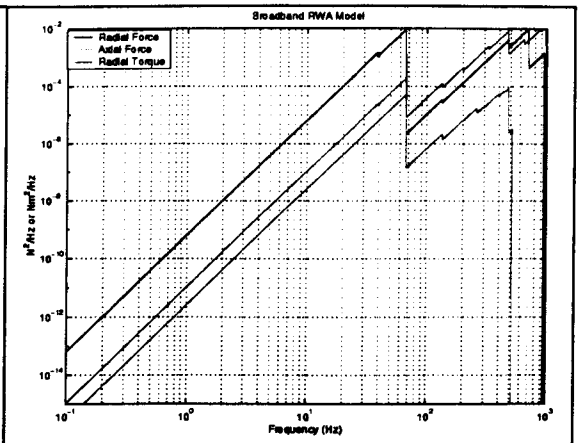

Figure 5b RWA broadband frequency PSD for three disturbance directions.

Figure 5b shows the broadband PSD's for the three axes of the disturbance for a single RWA. The stochastic broadband model is based on the discrete frequency model and assumes the wheel speed is a uniform random variable over the interval
10-66 rps (expected operating range). This approach facilitates the broadband frequency design and analysis by leading to a frequency domain model that can be propagated through the SIM integrated model to obtain the estimates of the OPD performance metrics. After the disturbance models are built, the transfer functions obtained from the SIM integrated model are input to the disturbance algorithm in order to determine the OPD as a function of the wheel speed and frequency. These performance metrics are commonly used in SIM Project to address the OPD jitter as a function of the wheel speed. Currently, SIM Reference Design requires 3 wheels on three different isolators aligned with the three axes of the spacecraft. For the simplicity, one raw and isolator pair along the z axis of the spacecraft was chosen to generate the disturbance transfer functions and then the contribution of the other wheels were added in the post processing using MATLAB routines.

Each transfer function obtained from the IMOS model of SIM Reference Design maps the contribution of that particular force or torque direction to OPD as a function of frequency. Since a reaction wheel contain disturbances in three force directions and two torque directions, the contributions of all these disturbances to the OPD jitter is determined using linear superposition. The OPD performance PSD can be written as [13]:

$$\Phi_{OPD}(\omega) = \sum_{j=1}^{5} \left|H_j(\omega)\right|^2 \left[\Phi_m\right]_j(\omega) \qquad (8)$$

where $\left|H_j(\omega)\right|^2$ is the transfer function relating the particular disturbance force or torque to OPD and $\left[\Phi_m\right]_j(\omega)$ is the PSD of the corresponding force or torque.

Both discrete and broadband approaches use the principal of superposition for the estimation of the OPD performance. The area under the discrete performance PSD gives the OPD variance for a given wheel speed. The broadband performance PSD is a continuous function of the frequency and numerical integration under the curve yields the mean square value of the performance where the integration limits are defined as 10-66 rps [14]. These two disturbance analysis methods are used in the following section to predict the OPD performance metrics of the SIM Reference Design. These methods provide valuable information to identify the design margins for the structure and the control system.

3. RESULTS

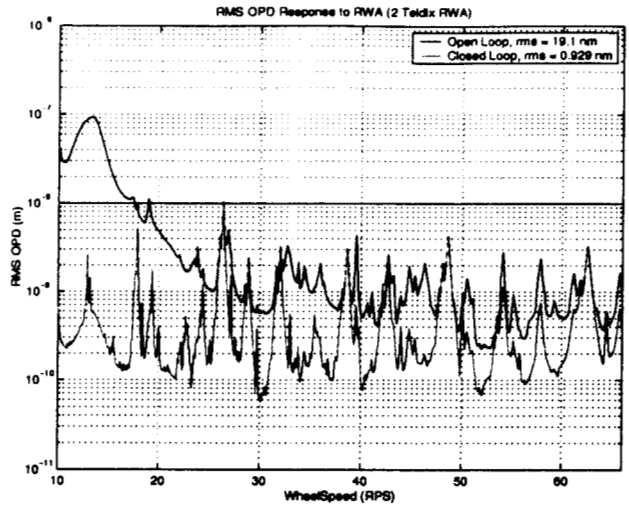

Figure 6 OPD variation as a function of wheel speed (rps).

OPD standard deviation was calculated at every wheel speed by taking the square root of the variance at that particular wheel speed. The OPD variation for the first interferometer as a function of the wheel speed is shown in Figure 6 for the open and closed loop configurations. The nominal metric, the root-mean square (rms) of the overall wheel speeds between 10-66 rps is also provided in the legend box. These results were obtained using the discrete frequency disturbance model running the wheel speed at every 60 rps. The requirement for SIM is shown on the plot with a straight solid line at 10 nm. As it can be seen from the figure, SIM Reference Design meets the 10 nm requirement for the open loop configuration for the overall wheel speeds other than the 14 rps. This peak is the main contributor to the rms OPD for the open loop configuration and loses its significance when the loops are closed. When the open and closed loop performances are compared above 20-66 rps, the control system does not attenuate the significant peaks at this region. This is an indication of existence of significant dynamics above 100 Hz which is excited by the unfiltered RWA disturbance forces.

The OPD performance prediction in Figure 6 presents the effect of all the harmonics as it is indicated in Eq. 7. When the RWA model has more than one harmonic, it is difficult to map the results in Figure 6 to the frequency domain. To investigate the multiple harmonic effect, the analysis was modified to include the contribution of each harmonic separately. Open loop and closed loop results from Figure 6 are also plotted in Figures 7 & 8, respectively, with a solid black line to make the comparison possible. TELDIX/RDR-68 wheel includes 19 harmonics and only first 12 are shown in the analysis. The open loop configuration in Figure 7 shows that the subharmonic (hi=0.58) excites the ~7 Hz mode of the RWA isolator. The frequency information was calculated by multiplying the harmonic number by the wheel speed ($h_i f_{rwa}$), and then this specific component mode was identified by animating the modeshapes at that frequency. One can use the same approach to extract the frequency information from Figure 8 for the closed loop configuration. Most of the significant peaks between 20 to 66 rps are due to the dynamics around ~180 Hz. This is also justified by plotting the broadband frequency PSD and cumulative rms plots in Figure 9. Steps in cumulative rms indicate the significant modes to OPD response. The metrology boom (1.2 Hz), delay line (3.5 Hz) and reaction wheel isolator (7 Hz) modes contribute the cumulative rms. For the open loop case all the rms contribution occurs below 100 Hz whereas for the closed loop configuration the 180 Hz peak contributes a significant amount to the total rms value.

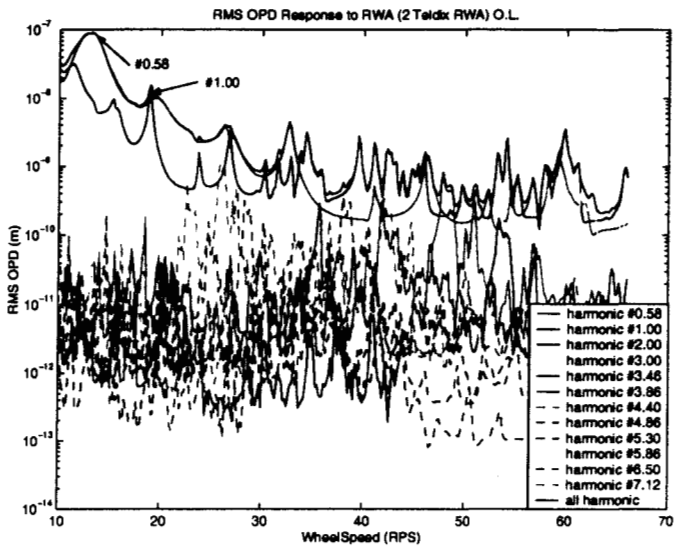

Figure 7 OPD variation for the open loop configuration showing the contribution of the first 12 harmonics.

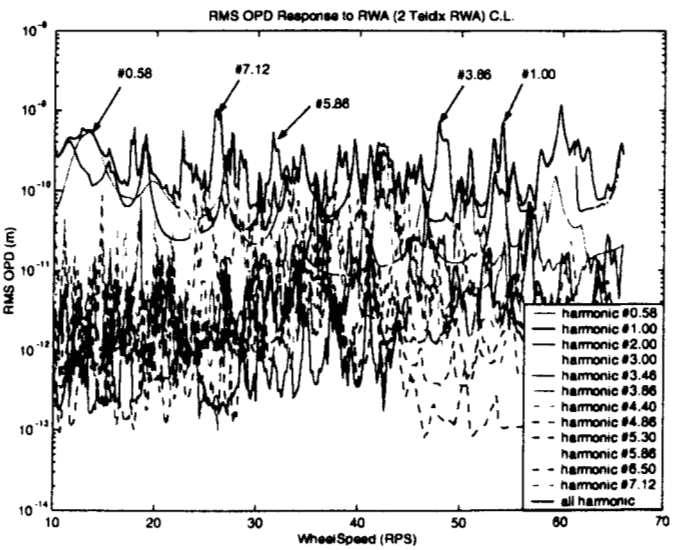

Figure 8 OPD variation for the closed loop configuration showing the contribution of the first 12 harmonics.

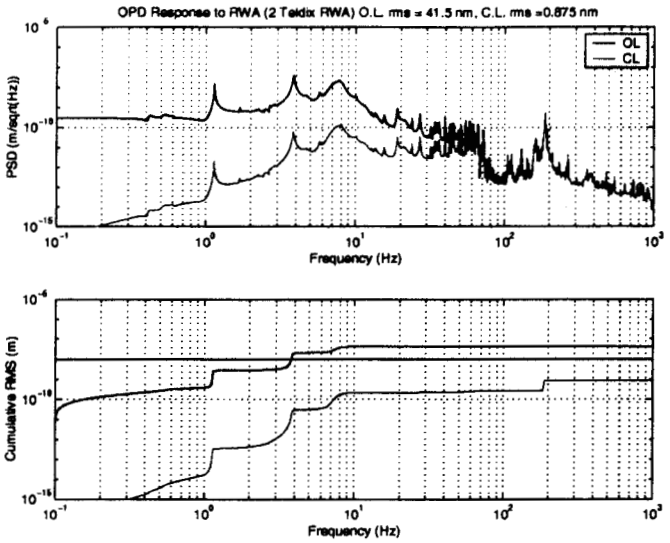

Figure 9 Broadband PSD and cumulative rms for the open loop and closed configurations.

Further analysis is needed to identify the sources of the dynamics at 180 Hz. It was a significant peak in the transfer functions (refer to Figure 3) but it's contribution to OPD was not evident until the disturbance analysis study was completed. Since it is beyond the bandwidth of the control system and is excited by the RWA disturbances at almost every wheel speed, a modification in the structural design may be considered at that frequency region.

Although the preliminary results show that SIM Reference Design meets the requirements for the overall wheel speeds, some of the component modeling assumptions have to be revisited and validated by supporting experimental studies. One of the likely sources of the error may be due to the ideal isolator models used to represent the RWA and backpack isolators. These passive isolators are modeled with corner frequencies around 7 Hz and an attenuation characteristic that falls 40 dB/decade. This may be not be representing the actual dynamics of these structures at high frequencies. Another issue that is being currently studied at JPL is the dynamic coupling between the RWA and the spacecraft. The impedance of the spacecraft at the location of the RWA will be different from that which the wheel sees during the rigid-based tests. Consequently, the actual disturbance entering the spacecraft might not be the same as what is modeled. Truly coupled accurate models are needed to represent the actual behavior of these components when they are assembled with large-scale flexible structures.

4. CONCLUSION

This paper summarizes the Integrated Modeling methodology and analysis tools used to predict the optical performance of the SIM Reference Design. A state space form of a combined structural and optical model was built to represent the dynamics of the instrument and the spacecraft. The disturbance models of the TELDIX/RDR-68 wheels were propagated through the transfer functions of the integrated model to obtain the performance metrics. The discrete frequency disturbance analysis method allows the assessment of the optical performance as a function of the wheel speed. This method was extended by showing the contribution of the different harmonics and identifying the critical modes of the structure that were excited by the RWA disturbances. The broadband frequency analysis was utilized as another method of examining the frequency domain to justify the conclusions derived from the discrete disturbance analysis. Preliminary results show that the current SIM Reference Design meets the mission requirements under the effect of RWA disturbances. However, the limitations and the accuracy of the modeling assumptions are being investigated as an ongoing study. Additional experimental studies are required for the validation of some of the component models such as the RWA isolators and the RWA disturbance models. Disturbances such as the sensor and actuator noises must be also incorporated in the integrated model together with the actual control system model for the future performance prediction studies.

The integrated modeling methodology is proven to be a valuable tool to predict the instrument performance before the flight system hardware is built. The methodology allows the navigation of the complex trade space for optimizing the performance of the instrument and enhancing the structural and control design.

5. ACKNOWLEDGEMENTS

The work described in this paper was carried out at the Jet Propulsion Laboratory, California Institute of Technology, under contract with the National Aeronautics and Space Administration.

6. REFERENCES

[1] M. M. Colavita, M. Shao, and M. D. Rayman, "Orbiting stellar interferometer for astrometry and imaging," *Applied Optics*, vol. 32, no. 10, pp. 1789-1797, April 1993.

[2] M. Shao and D. M Wolf, "Orbiting stellar interferometer," *Proceedings of SPIE Symposium on*

Spaceborne Interferometry, vol. 2447, (Orlando, FL), pp. 228-239, April 1995.

[3] Robert L. Grogan and R. A. Laskin, "On Multidisciplinary Modeling Of The Space Interferometry Mission," *Proceedings of the 1998 American Controls Conference*, Philadelphia, PA, June 1998.

[4] J. W. Melody and G. W. Neat, "Integrated modeling methodology validation using the micro-precision interferometer testbed," *Proceedings of 35th IEEE Conference on Decision and Control*, vol. 4, (Kobe, Japan), pp. 4222-4227, Dec 1996.

[5] I. Basdogan, F. Dekens, and G. W. Neat, " An Integrated Model Validation Study of the Wave Front Tip/Tilt System Using the Micro-Precision Interferometer Testbed," *Proceedings of 1999 IEEE Aerospace Conference*, Snowmass, CO, April 1999.

[6] M. H. Milman, H. C. Briggs, W. Ledeboer, J. W. Melody, R. L. Norton, and L. Needels, *Integrated Modeling of Optical Systems User's Manual, Release 2.0*, Nov. 1995. JPL D-13040.

[7] D. Redding, *Controlled Optics Modeling Package User Manual, Release 1.0*, June 1992. JPL D-9816.

[8] A. A. Shabana, *Theory of Vibration*, vol. 2, Springer-Verlag, 1991.

[9] M. B. Levine-West and J. W. Melody, "Model updating of evolutionary structures," *Proceedings of 15th ASME Biennial Conference on Mechanical Vibration and Noise*, (Boston, MA), Sept. 1995.

[10] G. W. Neat, A. Abramovici, J. W. Melody, R. J. Calvet, N. M. Nerheim, and J. F. O'Brien, "Control technology readiness for spaceborne optical interferometer missions, " *Proceedings of Space Microdynamics and Accurate Control Symposium*, (Toulouse, France), May 1997.

[11] R. Masterson, "Development and Validation of Empirical and Analytical, Master's thesis, Massachusetts Institute of Technology, June 1999.

[12] J. W. Melody, "Discrete-frequency and broadband reaction wheel disturbance models," Interoffice Memorandum 3411-95-200csi, Jet Propulsion Laboratory, June 1995.

[13] J. F. O'Brien, R. Goullioud, and G. W. Neat, "Micro-Precision Interferometer: Evaluation of new disturbance isolation solutions," SPIE Conference, San Diego, March 1998.

[14] H. L. Gutierrez, "Performance Assessment and Enhancement of Precision Controlled Structures During Conceptual Design," Ph.D. thesis, Massachusetts Institute of Technology, February 1999.

[15] R. Masterson, Reaction Wheel Data Analysis and Disturbance Modeling Toolbox, November 20, 1998.